

# Investigating Electromagnetic Surface Waves in Nonlinear Metamaterial Waveguide Structures Near the Dirac Point

Khitam Elwasife

Physics Department, Islamic University of Gaza, P.O. Box 108, Gaza, Palestinian Authority

Email: kelwasife[at]iugaza.edu.ps

**Abstract:** *This study theoretically examines electromagnetic surface waves in a nonlinear dielectric film bounded by a ferrite cover and negative zero positive index metamaterial substrate. The results, expressed in terms of the systems physical parameters, reveal that the proposed waveguide structures refractive index can be efficiently controlled by tuning the operating frequency. This research contributes to our understanding of surface waveguides and their potential applications in guided wave optics and integral optics*

**Keywords:** waveguide structure, nonlinear, ferrite, metamaterial, Dirac Point, electromagnetic surface waves, refractive index, operating frequency

## 1. Introduction

At present, LHM attract a growing interest of both theoretical and experimental research. In 1968, Veselago [1] suggested, that electromagnetic propagation in an isotropic medium with negative dielectric permittivity  $\epsilon(\omega) < 0$  and negative permeability  $\mu(\omega) < 0$  can exhibit unusual properties, Metamaterials are artificial media, in which man-made structural units play the role of atoms. Thus, the complex phenomena in metamaterials result from the characteristics of the individual elements as well as from the way they are arranged in a lattice. In other words, metamaterials gain emerging properties that were not available in their constitutive elements alone. This provides enormous flexibility in tailoring the response of metamaterials to external waves or fields. Shadrivov et al. [2, 3] proposed nonlinear LHM structure, a nonlinear guided modes in a waveguide formed by a slab of linear LHM embedded into nonlinear dielectric are studied, and shown that symmetric, antisymmetric and asymmetric waves are supported by such a waveguide, it has been predicted, that in nonlinear regime additional modes which do not exist in linear problem appeared. Podolskiy et al [4] have been proposed nonmagnetic linear LHM. Additionally, it was shown that photonic crystals demonstrate negative refraction under some conditions [5]. Recent studies of the waveguiding by the structures with LHMs have shown that the properties of guided modes in such systems differ essentially from those of conventional waveguides. So far, linear waves guided by an interface and by a slab of LHM [6, 7], as well as nonlinear surface waves [8] have been studied. It has been shown that the mode structure and frequency dispersion may have an unconventional form and unexpected properties. The behavior of electromagnetic waves propagating along the interface between a linear substrate and a nonlinear cladding, (when the materials involved magnetic materials with an external magnetic field) is analyzed. The dispersion relations for electromagnetic surface waves are derived [9]. Boardman and Egan [10] have investigated theoretically a nonlinear surface and guided polaritons for three nonlinear media. The polaritons describe as coupled mode which is an admixture of

electromagnetic field and elementary excitation in the medium that produce the resonance. Such electromagnetic waves are called polariton. It propagates along the surface of a medium, or along the interface between two media. Several novel optical transport properties near the dirac point (DP) have been investigated, such as conical diffraction [11]. Takumi Kaneda et al has been evaluated the Dual-band composite left-handed transmission lines with the nonreciprocal phase shift approximately proportional to the operating frequency are studied and using normally magnetized ferrite microstrip lines [12]. Numerical simulation results produced that the phase gradient of the fields along the resonator is controlled by the applied dc magnetic field to the ferrite, when studied a normally magnetized ferrite microstrip line-based composite left-handed material and ferrite structure transmission line as a metamaterial with variable phase-shifting nonreciprocity [13].

In this work we have investigated and computed the dispersion relation of nonlinear electromagnetic surface waves in a structure consisting of nonlinear film that bounded by Ferrite cover and a NZPIM substrate.

## 2. Theory

The structure have been considered as a simple one of multi structure. The propagation characteristics in the below three layers can be tuned and controlled by selecting the film thickness.

Figure (1) shows the coordinate system used, we shall assume that the nonlinear film occupies the region  $0 \leq z \leq h$ , bounded by the Ferrite cover of space  $z \geq h$  and bounded by NZPIM substrate.

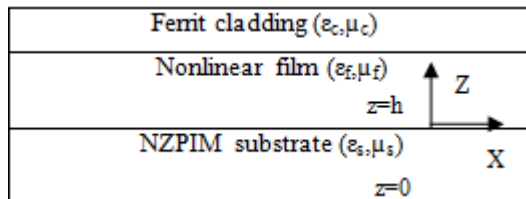


Figure 1: Nonlinear waveguide bounded by Ferrite cover and NZPIM substrate

The stationary solutions of the TE wave equation have the form  $E_y(z)\exp(ik_x - \omega t)$ , where the amplitude  $E_y(z)$  is real,  $k_x$  is the propagation constant along the longitudinal direction and  $\omega$  is the frequency of the wave. Using this form of the stationary solution, Maxwell's equations can be written as

$$\frac{\partial^2 E_y(z)}{\partial z^2} + (k_0^2 \epsilon_i \mu_i - k_x^2) E_y(z) = 0 \quad (1)$$

where  $k_0$  is the free space wave number,  $i = s, f,$  or  $c$  indicating the substrate, film and cladding, and  $k_x = k_0 N$  with  $N$  is the modal index of the propagating mode. If the optical nonlinearity is of the Kerr-type, then the dielectric constant of the film is

$\epsilon_f + \alpha_f |E_f|^2$ , that is  $\alpha_f$  is the nonlinear coefficient. In our a model  $\epsilon_s$  and  $\mu_s$  of the LHM take the form

$$\epsilon_s(\omega) = 1 - \frac{\omega_{ep}^2}{\omega^2 + i\gamma_e \omega}, \mu_s = 1 - \frac{\omega_{em}^2}{\omega^2 + i\gamma_m \omega} \quad (2)$$

for the NZPIM  $\omega_{ep}^2$  and  $\omega_{em}^2$  are the electronic and magnetic plasma frequencies, and  $\gamma_e$  and  $\gamma_m$  are the damping rates relating to the absorption of the material.

$$\text{where } k_s^2 = k_x^2 - \omega^2 \mu_o \epsilon_o \epsilon_s, k_c^2 = k_x^2 - \omega^2 \mu_o \epsilon_o \epsilon_c, p = \sqrt{(q^2 + k_f^2) / 2\Lambda_f}$$

$$q = (k_f^4 + 4 \wedge_f C_f)^{1/4}, \Lambda_f = \frac{\omega^2 \alpha_f}{2c^2}, G = \frac{cq}{\omega}, n_i^2 = (n_x^2 - \epsilon_i), i = s, f, c$$

$$n_x = \frac{ck_x}{\omega}, (op)_0 = \left( \frac{\alpha_f E_o^2}{2} \right), (op)_h = \left( \frac{\alpha_f E_h^2}{2} \right)$$

The constants  $E_o$  and  $E_h$ , represent the value of the electric field at the lower and upper boundary of the film. The nonzero magnetic field components ( $H_x$  and  $H_z$ ) of the TE modes can be The boundary conditions require that the tangential components of E and H be continuous at  $z = 0$  and

The two claddings marked with region s (substrate) and region c (cladding) have parameters ( $\epsilon_s$  and  $\mu_s$ ) and ( $\epsilon_c$  and  $\mu_c$ ), respectively. The cladding is assumed to be a gyromagnetic ferrite layer which is described by a magnetic permeability tensor as [14-16].

$$\mu(\omega) = \begin{bmatrix} \mu_{xx} & 0 & \mu_{xz} \\ 0 & \mu_B & 0 \\ -\mu_{xz} & 0 & -\mu_{xx} \end{bmatrix}$$

Where

$$\mu_{xx} = \mu_B \left( \frac{\omega_0(\omega_0 + \omega_m) - \omega^2}{\omega_0^2 - \omega^2} \right), \mu_{xz} = i\mu_B \frac{\omega\omega_m}{\omega_0^2 - \omega^2} \quad (3)$$

And  $\mu_B = \mu_{xx} + \frac{\mu_{xz}^2}{\mu_{xx}}$  with  $\mu_B$  is the usual Polder tensor

element,  $\omega_0 = \gamma_f \mu_0 H_0$ ,  $\omega_m = \gamma_f \mu_0 M_0$ ,  $H_0$  is the DC applied magnetic field,  $\gamma_f$  is the gyromagnetic ratio,  $M_0$  is the DC magnetization of the magnetic insulator. The solution of Eq. (1) in the three-layer structure is given by

$$E_y^{(s)} = E_o \exp(k_s z) \quad (4)$$

$$E_y^{(f)} = P \text{cn} [q(z + z_o) | m] \quad (5)$$

$$E_y^{(c)} = E_h \exp[K_c (h - z)] \quad (6)$$

$z = h$ , yielding a set of homogeneous linear equations for the coefficients  $E_o$  and  $E_h$ . The determinant of this set must be zero for nontrivial solution to exist. After some manipulations, the following dispersion relation for TE surface waves is obtained.

$$\frac{4(op)_0 (op)_h}{\alpha_f E_o E_h} = \frac{cn[qh] \{ (n_x^2 - \epsilon_s \mu_s)(op)_0 + (n_x^2 - \epsilon_c \mu_c)(op)_h + G^2((op)_0 + (op)_h) + ((op)_0 - (op)_h) \}}{(G^2 - \sqrt{n_x^2 - \epsilon_s \mu_s} \sqrt{n_x^2 - \epsilon_c \mu_c})} \quad (7)$$

Where  $n_x$  is the refractive index,  $(op)_0$  and  $(op)_h$  are the optical power densities

### 3. Numerical Results and Discussion

In order to study the dispersion characteristics of the proposed structure, the dispersion relation has to be solved numerically to find the effective refractive index  $N(x)$  as a function of power density. The numerical calculations were

carried out with the same parameters for the ferrite (YIG) substrate as [17-19]. Here we assume  $\gamma_e$  and  $\gamma_m = \gamma << \omega_{ep}^2, \omega_{mp}^2$  respectively. It is important that when  $\omega_{ep} = \omega_{em} = \omega_D$ , where  $\omega_D$  is the frequency of the optical DP (corresponding

wavelength is  $\lambda_D = (2\pi c/\omega_D)$ , where two bands touch each other forming a double cone structure, and  $\gamma = 0$  (no loss), then  $\epsilon_s = \mu_s = 1 - \omega_D^2/\omega^2$  Which indicates both  $\epsilon_s(\omega_D)$  and  $\mu_s(\omega_D)$  may be zero simultaneously.  $\omega_D = (\omega/0.8)$  is the frequency of the optical DP (corresponding wavelength is  $\lambda_D = 2\pi c/\omega_D$ ), where two bands touch each other forming a double cone structure. In this case, the linear dispersion near the DP,  $\omega \approx \omega_D$ . Figure (1) illustrate Dispersion curves of TE-polarized surface waves for different thickness where  $h=3.1 \mu\text{m}$ ,  $h=2.9 \mu\text{m}$ , and  $h=2.8 \mu\text{m}$  in three curves respectively and  $b=.4$ ,  $\omega_0 = 4.0 \text{ GHz}$ , power density = 3,  $\omega_3 = 1$ ,  $\gamma_f = 1.76 \times 10^{11} \text{ s}^{-1}\text{T}^{-1}$ ,  $\mu_0 M = 0.175 \text{ T}$ , and  $\mu_0 H_0 = 0.5$ . For decreasing thickness the power density is increased. The existence regions of the nonlinear surface waves also depend on the frequency properties and the nonlinear value  $(op)_0$  as shown in Figure (2). It clear from the curve that the different optical power density  $(op)_0 = 0.4$ ,  $(op)_0 = 0.3$ ,  $(op)_0 = 0.2$ , and  $(op)_0 = 0.18$ , respectively for  $(op)_0 = .4$ ,  $\omega_0 = 4.0 \text{ GHz}$ ,  $\epsilon_3 = 1$ ,  $\gamma_f = 1.76 \times 10^{11} \text{ s}^{-1}\text{T}^{-1}$ ,  $\mu_0 M = 0.175 \text{ T}$ , and  $\mu_0 H_0 = 0.5$ .

We further show the unique properties of nonlinear surface wave near DP in the nonlinear NZPIM waveguide with the angular frequency varying from  $\omega < \omega_D$  to  $\omega > \omega_D$ . In Fig. 3. Dispersion curves of TE-polarized surface waves for different frequencies curve(1),  $\omega=103.4\text{GHz}$ , curve(2),  $\omega =103.5\text{GHz}$  and curve(3),  $\omega=103.55\text{GHz}$ ,  $(op)_0=0.2$ , respectively for  $(op)_h=.4$ ,  $\omega_0 = 4.0 \text{ GHz}$ ,  $(op)_0=0.2$ ,  $\epsilon_3 = 1$ ,  $\gamma_f = 1.76 \times 10^{11} \text{ s}^{-1}\text{T}^{-1}$ ,  $\mu_0 M = 0.175 \text{ T}$ ,  $\mu_0 H_0 = 0.5$  and  $\omega_D = \omega/0.8$ , we show that the refractive index increased by increasing the frequency by 0.05 GHz, and there is smoothly directly proportional between the thickness of film and frequency. Fig. 4. Represent the curve between refractive index and film thickness by changing the dirac frequency, Fig .5. is the dispersion curves of TE-polarized surface waves for different power density curve(1)  $(op)_0 = 0.4$  curve(2)  $(op)_0 = 0.3$ , respectively, for  $(op)_0 = .4$ ,  $\omega_0 = 4.0 \text{ GHz}$ ,  $(op)_0 = 3$ ,  $\epsilon_3 = 1$ ,  $\gamma_f = 1.76 \times 10^{11} \text{ s}^{-1}\text{T}^{-1}$ ,  $\mu_0 M = 0.175 \text{ T}$ ,  $\mu_0 H_0$  and  $\omega_D = 0.05\omega$ .

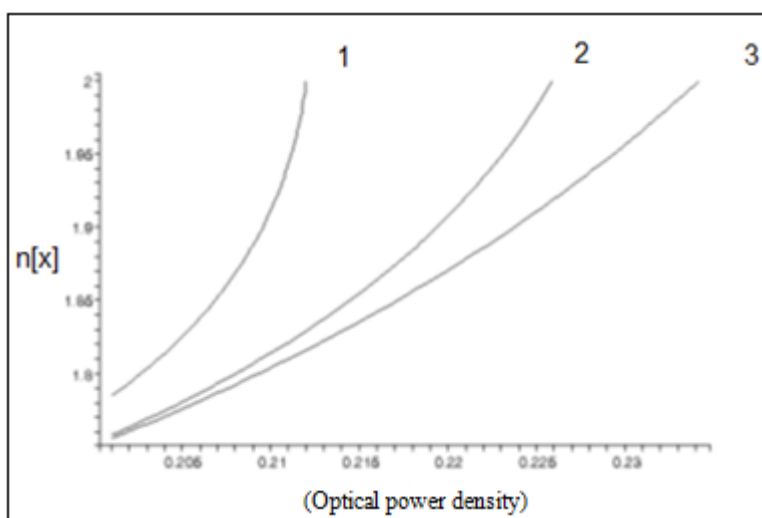


**Figure 2:** Dispersion curves of TE-polarized surface waves for different thickness curve(1)=  $h=3.1 \mu\text{m}$  curve(2),  $h=2.9 \mu\text{m}$ , curve(3),  $h=2.8 \mu\text{m}$  respectively for  $(op)_h=.4$ ,  $\omega_0 = 4.0 \text{ GHz}$ ,  $(op)_0$  optical power density = 0.3,  $\epsilon_3 = 1$ ,  $\gamma_f = 1.76 \times 10^{11} \text{ s}^{-1}\text{T}^{-1}$ ,  $\mu_0 M = 0.175 \text{ T}$ ,  $\mu_0 H_0 = .5$ , and  $\omega_D = \omega/0.8$

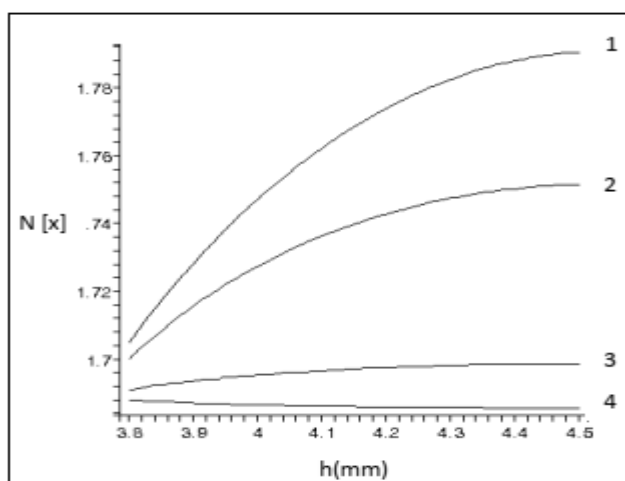


**Figure 3:** Dispersion curves of TE-polarized surface waves for different power density curve(1)  $(op)_0 = 0.4$  curve(2)  $(op)_0 = 0.3$ , curve(3)  $(op)_0 = 0.2$ , curve (4)  $(op)_0 = 0.18$ , respectively, for  $(op)_0 = .4$ ,  $\omega_0 = 4.0 \text{ GHz}$ ,  $(op)_0 = 3$ ,  $\epsilon_3 = 1$ ,  $\gamma_f = 1.76 \times 10^{11} \text{ s}^{-1}\text{T}^{-1}$ ,  $\mu_0 M = 0.175 \text{ T}$ ,  $\mu_0 H_0 = 0.5$  and  $\omega_D = \omega/0.8$

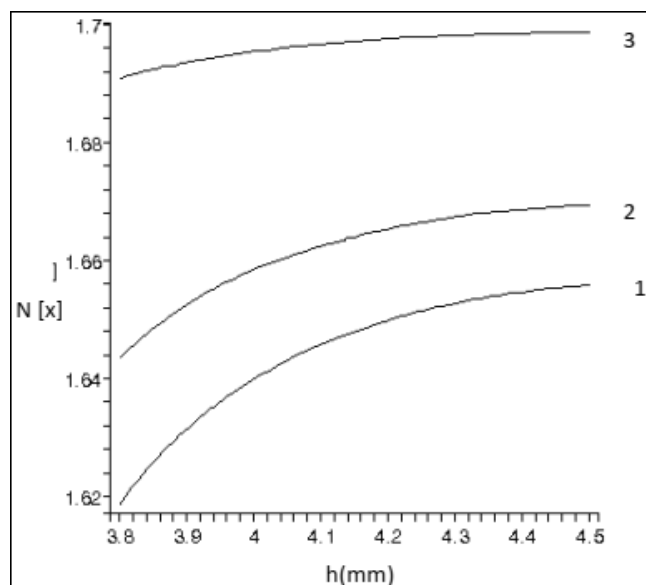


**Figure 4:** Dispersion curves of TE-polarized surface waves for different frequencies curve(1)  $\omega=103.4\text{GHz}$ , curve(2)  $\omega =103.5\text{GHz}$ , curve(3)  $\omega=103.55\text{GHz}$ ,  $(op)_0=0.2$ , respectively

for  $(op)_h=4$ ,  $\omega_0 = 4.0$  GHz,  $(op)_0=0.2$ ,  $\epsilon_3 = 1$ ,  $\gamma_f = 1.76 \times 10^{11} \text{ s}^{-1}\text{T}^{-1}$ ,  $\mu_0 M = 0.175$  T,  $\mu_0 H_0 = 0.5$  and  $\omega_D = \omega/0.8$

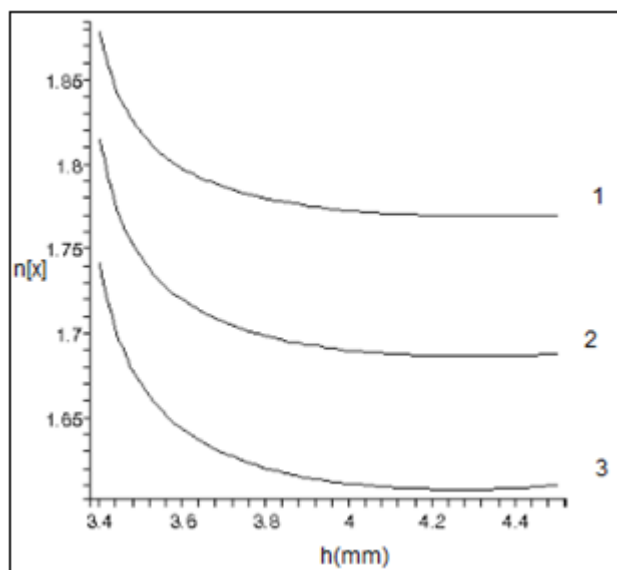


**Figure 5:** Dispersion curves of TE-polarized surface waves for different  $\Omega[d]$  curve(1)  $\omega_d = \omega/0.8$ , curve(2)  $\omega_d = \omega/0.81$ , curve(3),  $\omega_d = \omega/0.82$ ,  $(op)_0 = 0.2$ , respectively for  $(op)_0$ ,  $b = 4$ ,  $\omega = 103.2$ , GHz  $\omega_0 = 4.0$  GHz,  $(op)_0 = 0.2$ ,  $\epsilon_3 = 1$ ,  $\gamma_f = 1.76 \times 10^{11} \text{ s}^{-1}\text{T}^{-1}$ ,  $\mu_0 M = 0.175$  T,  $\mu_0 H_0 = 0.5$  and  $\omega_D = \omega/0.8$

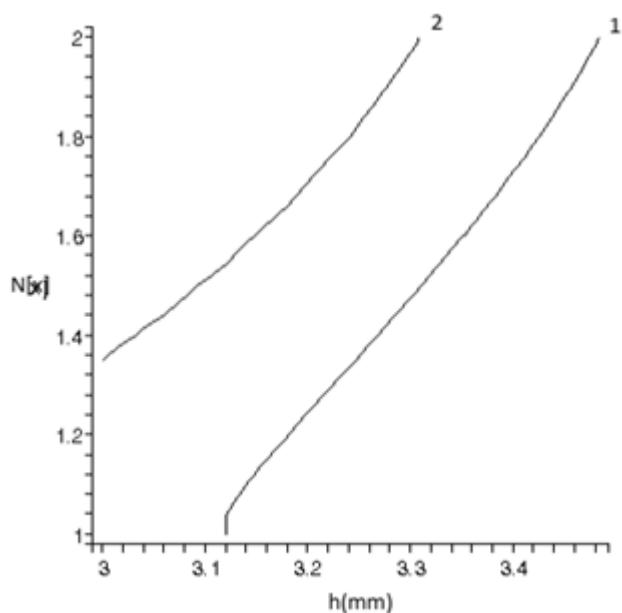


**Figure 6:** Dispersion curves of TE-polarized surface waves for different power density curve(1)  $(op)_0 = 0.4$  curve(2)  $(op)_0 = 0.3$ , respectively, for  $(op)_0 = 4$ ,  $\omega_0 = 4.0$  GHz,  $(op)_0 = 3$ ,  $\epsilon_3 = 1$ ,  $\gamma_f = 1.76 \times 10^{11} \text{ s}^{-1}\text{T}^{-1}$ ,  $\mu_0 M = 0.175$  T,  $\mu_0 H_0$  and  $\omega_D = 0.05$

#### 4. Conclusion

This study investigated the nonlinear plasmonics in NZPIM. The findings revealed that the refractive index of the proposed waveguide structure can be efficiently controlled by tuning the operating frequency. These results contribute to a deeper understanding of surface waveguides and their

potential applications in guided wave optics, integral optics, and optical based devices.

#### References

- [1] V. Veselago, **10**, 509 (1968).
- [2] V. Shadrivov, arXiv:physics, **2**, 126 (2003).
- [3] V. Shadrivov, arXiv of physics, **7**, 31 (2004).
- [4] A. Viktor, A. and E. Evgenii, Near-sighted superlens, *Physics*, **20**, 78 (2008).
- [5] M. Notomi, *Phys. Rev. B.*, **62**, 10696 (2000).
- [6] R. Ruppin, *Phys. Lett. A* **277**, 61 (2000).
- [7] I. V. Shadrivov, A. A. Sukhorukov, Yu. S. Kivshar, *Phys. Rev. E* **67**, 057602-4 (2003).
- [8] I. V. Shadrivov, A. A. Sukhorukov, Yu. S. Kivshar, A. A. Zharov, A. D. Boardman, and P. EgaarXiv:physics, **2**, (2003)
- [9] A.D. Boardman, A.D., M. Shabat. and R.F. Wallis R.F., *J. Phys. D: Appl. Phys.*, **24**, 1702 (1991).
- [10] A. D. Boardman and P. Egan *Journal De physique.* **45**, (1984).
- [11] O. Peleg, O. G. Bartal, G., Freedman, B.; Manela, O., Segev, M. & Christodoulides, D. N., *Phys. Rev. Lett.*, **98**, (2007).
- [12] T. Kaneda, & T. Ueda, Dual-band composite right/left-handed metamaterial lines with dynamically controllable nonreciprocal phase shift proportional to operating frequency. *Nanophotonics*, **11**, 2097-2106. (2022).
- [13] T. Ueda, M. Kamino, T. Kondo, Two-degree-of-freedom control of field distribution on nonreciprocal metamaterial-line resonators and its applications to polarization-plane-rotation and beam-scanning leaky-wave antennas. *IEEE Transactions on Microwave Theory and Techniques*, **70**, 50-61. (2021).
- [14] M. S. Hamada, "Non-Linear Surface Waves At a Single Interface of Semimagnetic Semiconductor – Left Handed Materials . *International Journal of Microwave and Optical Technology*, **2**, (2007).
- [15] R.W. Damon, and J.R. Eshbach, "Magnetostatic modes of ferromagnetic slab", *J. Phys. Ch. Solids*, **19**, 308 (1961).
- [16] M. M. Shabat, "Nonlinear Magnetostatic Surface Waves in a gyromagnetic film" *philosophical Magazine B*, **73**, 669 – 676, (1996).
- [17] S T Chui1, C T Chan2 and Z F Lin., *J. Phys.: Condens. Matter* **18** L89–L95, (2006).
- [18] Kh. Elwasife1, M. Mohammed M. Shabat, H. El Khozondar, *J. Mod. Phys.* **1**, 38-50, (2012).
- [19] K.Y. Elwasife, M.M. Shabat, S.S. Yassin , *An-Najah Univ. J. Res. (N. Sc.)*, **18**, 216-236, (2004).